MorphCT Results - Device Simulations

Matthew Jones

June 21, 2017

1 Test System

NOTE: We still don't have a real device morphology to work with, so I've bodged one together from the data we already have. It will not suffice for publication, but I'm hoping it will allow me to get all the moving parts in place before we set the code loose on a physical system

```
# Z = 9 + 1 ANODE
1 1 1 0 0 0 0 0 0
0 1 1 1 0 0 0 0 0
0 0 1 1 1 1 0 0 0
0 1 1 1 0 0 0 0 0
2 2 2 2 2 2 2 2 2
3 3 3 4 3 3 3 3 3
3 3 3 4 4 4 3 3 3
3 3 3 3 4 4 3 3 3
3 3 3 3 4 4 4 3 3
# Z = 0 - 1 CATHODE
```

Figure 1: A single slice of the test device used to write and configure the device-scale KMC code

ID	Simulation Name	XML Name	$l_{x,y,z}$ (Å)
0	orderedP3HT	p1-L15-f0.0-P0.1-T1.5-e0.5	85.19
1	disorderedP3HT	shrunkp1-L15-f0.0-P0.1-T2.0-e0.5	85.19
2	interfaceP3HTC60	p1-L15-f0.3-P0.1-T1.5-e0.1	96.23
3	disorderedPCBM	pcbm-0.5-P0.5-300-T3.0_AA	65.69
4	orderedPCBM	pcbm-0.5-P1.5-200-T5.0_AA	57.53

Table 1: The morphologies selected for use in each cell in the device. The ID integers correspond to 'moietyType', and '$l_{x,y,z}$' is the cubic box length for each molecular system.

- The device is a cube consisting of 9x9x9 Cartesian lattice of 'cells' or 'moieties', where each cell in the lattice corresponds to one $\sim$ 10 nm molecular morphology.

- The layout of a single x-z slice of the device is depicted in figure 1. Each cell is assigned an integer [0-4], which represents the molecular morphology type within as described in table 2.4. The structure is therefore a simple bilayer, with regions of crystalline donor and acceptor material in amongst the amorphous melt.

- 9 identical copies of the slice are combined in the y-direction to make the 3D structure.

- Note that the molecular morphology describing each of these cells is actually a different size. On average, each cell represents a structure that is cubic with side 7.8 nm, and so this value was used when calculating displacements within the device.

- Additionally, no orientational manipulation has been applied to these systems. That is, that all of the P3HT crystal cells in the system are identical and oriented the same way. Similarly, the interface cells (which form vertical lamellae of P3HT in the middle and C60 molecules aggregating around the outside) have not been rotated or manipulated in any way.

- The device is periodic in the x and y directions, but is capped at $Z = -1$ and $Z = 9$ by planes that describe the cathode and anode respectively. Carriers crossing into these planes are counted towards the generated photocurrent, and excitons are forbidden from hopping into them. Eventually, these planes will also consider dark-current injection which is vital for device operation.

2 Getting Excitons Working

Before including carrier hopping (which will require a calculation and treatment of coulombic and field effects etc.), it is important to get the exciton dynamics correct.

- Excitons are injected into the device according to the photoinjection rate:

$$k_{\text{photo}} = \Phi \frac{\lambda}{hc} A \left(1 - \exp^{-\alpha(z)}\right), \tag{1}$$

  where Φ is the incident flux (0.01 mW/cm^2), λ is the wavelength (500 nm), A is the photosensitive area (9 $\times$ 7.8 nm $\times$ 9 $\times$ 7.8 nm), and α is the thickness-dependent absorption coefficient (1.3×10^4 $\times$ 9 $\times$ 7.8 $\times10^{-9}$)

- This rate is converted to a wait time for the next photoinjection using the normal KMC algorithm, and then an exciton is placed in a random cell, on a random chromophore after the wait time.

- Only after the exciton has been injected is the next photoinjection wait time calculated.

- The exciton is then permitted to hop based on a modified Förster hopping rate:

$$k_{\text{FRET}} = \frac{B}{\tau_{\text{ex}}} \left(\frac{r_F}{r_{ij}}\right)^6, \tag{2}$$

  where τ_{ex} is the exciton lifetime parameter (0.5 ns), r_F is the Förster radius (4.3 nm), r_{ij} is the distance from the initial chromophore to the hop destination, and B is a coefficient that takes into account the Boltzmann energy penalty for hopping upstream in energy ($\exp^{-\Delta E_{ij}/k_B T}$ for $\Delta E_{ij} > 0$, and 1 for $\Delta E_{ij} \leq 0$), as well as a variable prefactor that will be discussed later.

- If an exciton hops to a chromophore that is within 1 nm of an opposing chromophore type (i.e. both a donor and an acceptor chromophore in range), it will instantaneously dissociate (removed from the system) to create an electron on the acceptor chromophore and a hole on the donor.

- Excitons also are given a lifetime, t_{ex} based on τ_{ex} ($t_{\text{ex}} = -\ln(x\tau_{\text{ex}})$, where x is a random number in the interval $[0, 1)$). If the exciton would hop for any time longer than t_{ex}, it is instead removed from the system and counted as recombining, without generating charge carriers.

Note that all subsequent data has been run using the same random number seed to ensure comparable statistics.

2.1 Prefactor $= 1 \times 10^0$

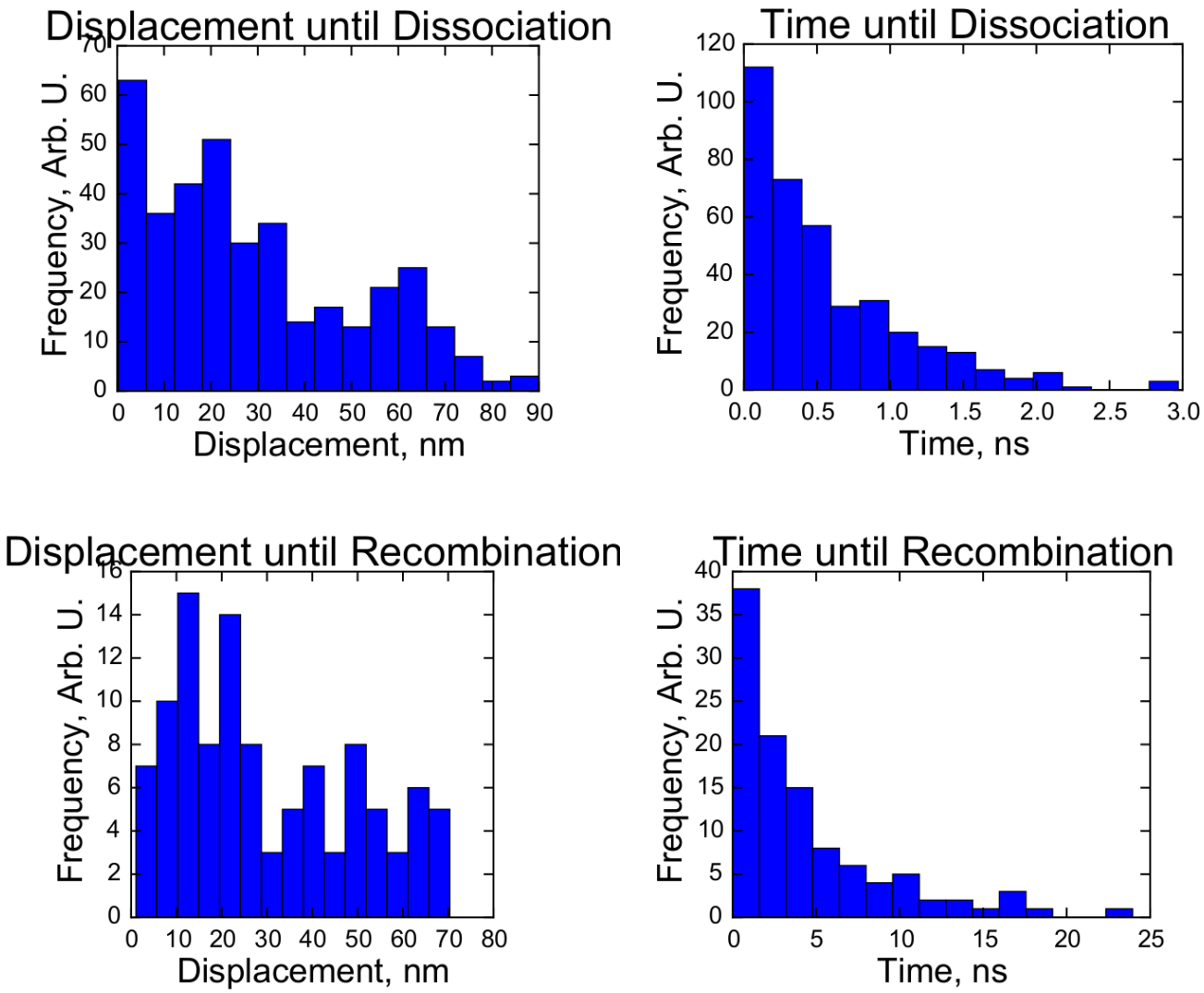

Figure 2: The measured exciton dynamics given a k_{FRET} prefactor of 1.0

- The above results incentivised the k_{FRET} equation modification as it seems to be unsuitable for describing this high-resolution exciton transport.
- Excitons are consistenly moving for many tens of nm, which is too high for this kind of organic system (somewhat based on P3HT:PCBM, which has a mean-free path length of around 5 nm.
- Additionally, the lifetimes of the non-dissociating excitons are far too high. The lifetime parameter should be restricting the lifetime to around 0.5 ns, not 20+.

- The driving factor in the equation is the $(\frac{r_F}{r_{ij}})^6$. r_{ij} is of the order angstroems, which forces the rate coefficient to be extremely high, allowing the exciton to move very far in a short space of time.
- As such, it might be a good idea to reduce the rate coefficient through the use of a prefactor, in order to get the expected exciton dynamics
- There is some partial justification in this according to Ref[1], which suggests that the intrinsic point-dipole assumption in FRET might not be suitable for some materials.
- This is a complicated issue though because Refs[1,2] also show diffusion lengths of around 40nm given 90 meV of energetic disorder and a Förster length of 4.3 nm, which isn't miles off.
- With a prefactor of 1.0, the exciton dissociation efficiency was 79% for our bilayer morphology.

2.2 Prefactor $= 1 \times 10^{-2}$

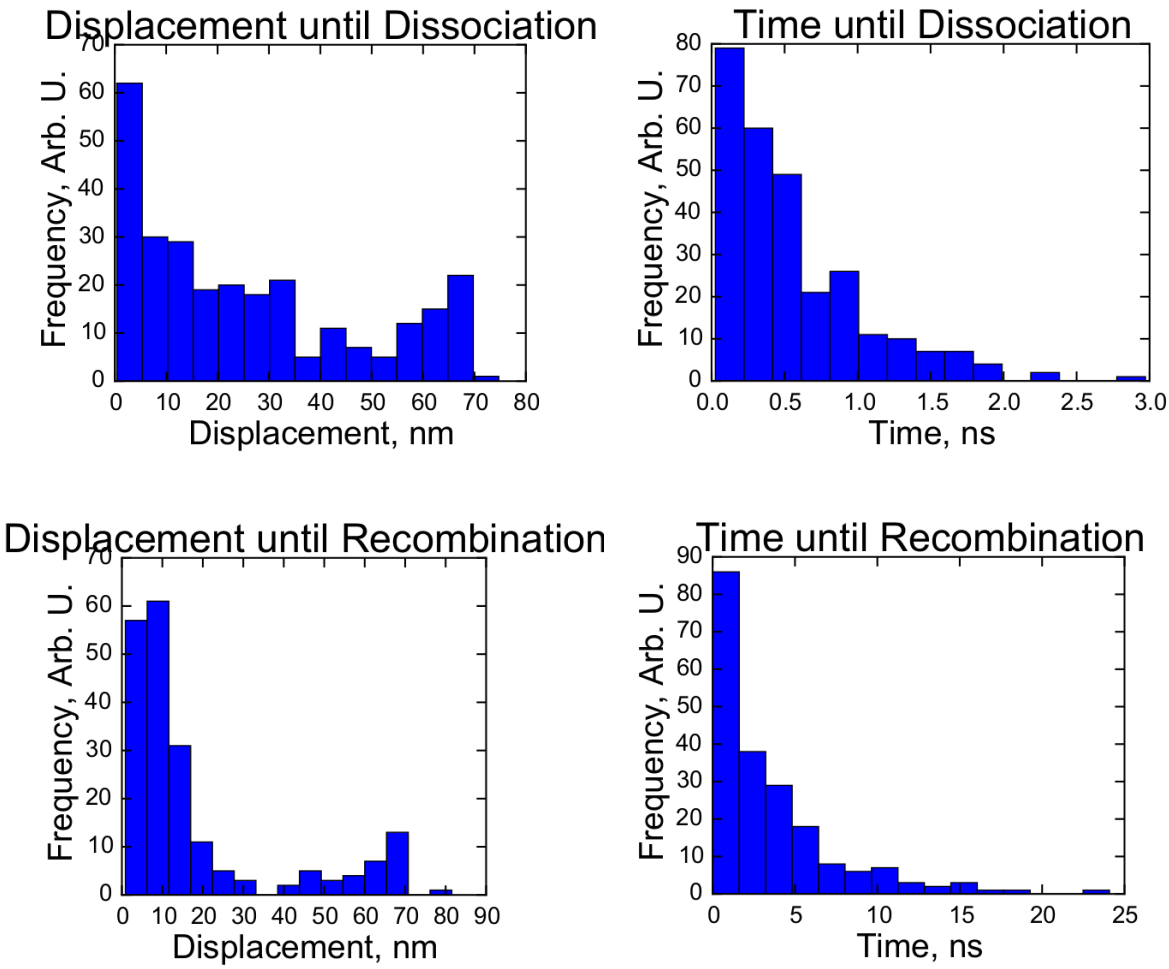

Figure 3: The measured exciton dynamics given a k_{FRET} prefactor of 0.01

- Reducing the FRET hopping rates by 2 orders of magnitude has improved the exciton dynamics slightly, as excitons travel less far before recombining. Around twice as many excitons are recombining within 0.5 ns, and the majority have a pre-recombination free path of less then 40 nm.
- With a prefactor of 0.01, the exciton dissociation efficiency was XX% for our bilayer morphology.

2.3 Prefactor $= 1 \times 10^{-4}$

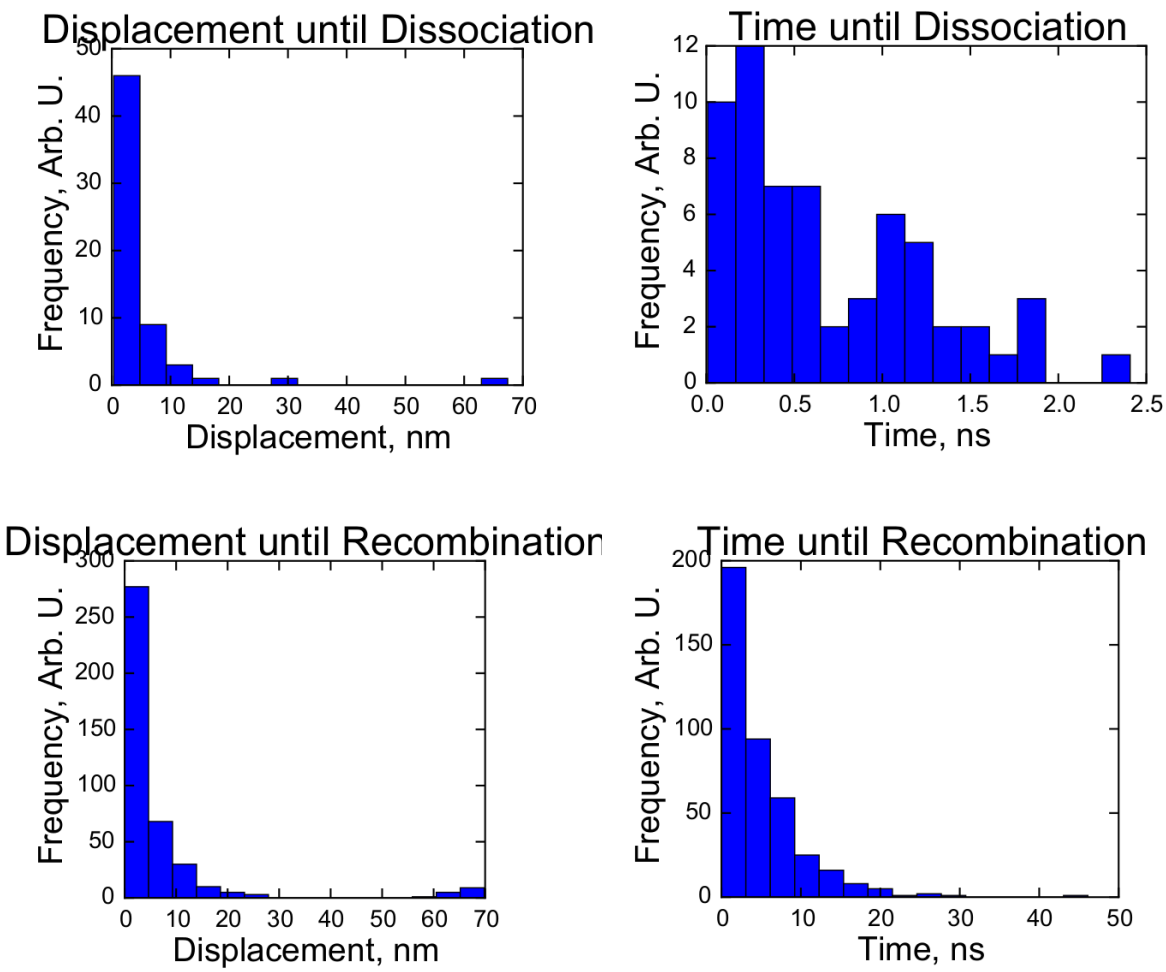

Figure 4: The measured exciton dynamics given a k_{FRET} prefactor of 0.0001

- Reducing the FRET hopping rates to 1×10^{-4} has affected the exciton dynamics more strongly, with nearly all excitons dissociating or recombining within 30 nm (except for a small few that are spawned in crystals and so can travel significantly further) and a few nanoseconds.
- With a prefactor of 1×10^{-4}, the exciton dissociation efficiency was 12.6% for our bilayer morphology.

2.4 Summary of Prefactor Investigation

Prefactor	Recombination		Dissociation		XDE
	Time (ns)	Disp (nm)	Time (ns)	Disp (nm)	%
1×10^{0}	0.45 ± 0.04	30 ± 2	0.57 ± 0.03	29 ± 1	77.8
1×10^{-2}	0.35 ± 0.03	18 ± 1	0.55 ± 0.03	26 ± 1	58.2
1×10^{-4}	0.48 ± 0.03	6.3 ± 0.6	0.69 ± 0.07	5 ± 1	12.6

Table 2: The morphologies selected for use in each cell in the device. The ID integers correspond to 'moietyType', and '$l_{x,y,z}$' is the cubic box length for each molecular system.

- Modifying the prefactor does not significantly affect the average recombination or dissociation time, however, it does strongly affect the distance that the exciton can travel.
- Additionally, it significantly reduces simulation runtime, which will be important during the full carrier-included device simulations as exciton transport is not expected to be the most computationally intensive part of the simulation.
- In order to obtain the 'correct' [CITATION NEEDED] path lengths for excitons in the sorts of systems that we are investigating, we should modify the Förster transport rate by a prefactor of 1×10^{-4} to ensure consistent exciton dynamics.

References

[1] Krishna Feron, Warwick Belcher, Christopher Fell, and Paul Dastoor. Organic Solar Cells: Understanding the Role of Förster Resonance Energy Transfer. *International Journal of Molecular Sciences*, 13(12):17019–17047, dec 2012.

[2] Stavros Athanasopoulos, Evguenia V. Emelianova, Alison B. Walker, and David Beljonne. Exciton diffusion in energetically disordered organic materials. *Physical Review B*, 80(19):195209, 2009.